The progression and global dispersion of the Hunga aerosol cloud, & influence from co-emitted water vapour, aligned to the APARC Hunga impacts report

Graham Mann[1,2], Sandip Dhomse[1,2,3], Bill Randel[7]

(1: School of Earth and Environment, University of Leeds, U.K.
2: National Centre for Atmospheric Science (NCAS-Climate) U.K.
3: National Centre for Earth Observation (NCEO), Univ. Leeds, U.K.)

(NCAR, Boulder, Co, USA)

Yunqian Zhu[4,5] Margot Clyne[5,6]

(4: National Ocean for Atmos. Admin, NOAA)
5: Univ. Colorado, 6: Colorado State Univ.)

Ghassan Taha[8,9]

(8: NASA Goddard Space Flight Center, USA
9: Morgan State Univ., Baltimore, USA)

Mathieu Colombier[10]

(10: Ludwig Maximilians-Univ, Munich, Germany

Paul Newman[11]

(11: NASA Goddard Space Flight Center, USA)

GA4 UM-UKCA model

Interactive strat-trop chemistry (CheST)
(Archibald et al., 2020)

Interactive aerosol microphysics
GLOMAP-mode
(Mann et al., 2010; 2012; Dhomse et al., 2014; 2020)

Internally generated QBO
within 85-level HadGEM3-A
(Osprey et al., 2013)

GA4 = precursor to UKESM

Same capability applied (no-MSP & evap'n-OFF) for
-- **UKESM interactive strat-aerosol CMIP6 historical**
(T. Aubry, Univ. Exeter)

-- **UKESM interactive strat-aerosol PMIP4 Last Millenium**
(L. Marshall, Univ. Durham)

3. UM-UKCA interactive stratospheric aerosol model

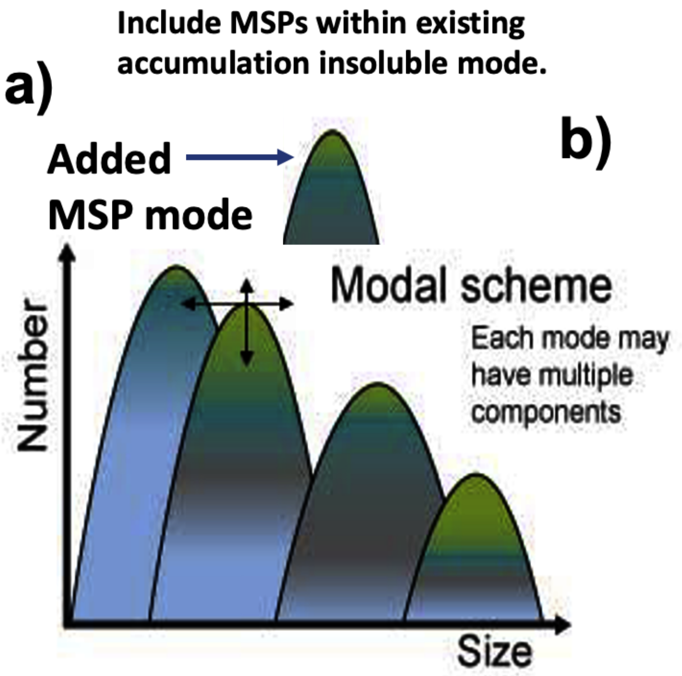

Fig 2a. Schematic of multi-modal size representation in GLOMAP-mode aerosol microphysics scheme (Mann et al., 2010)

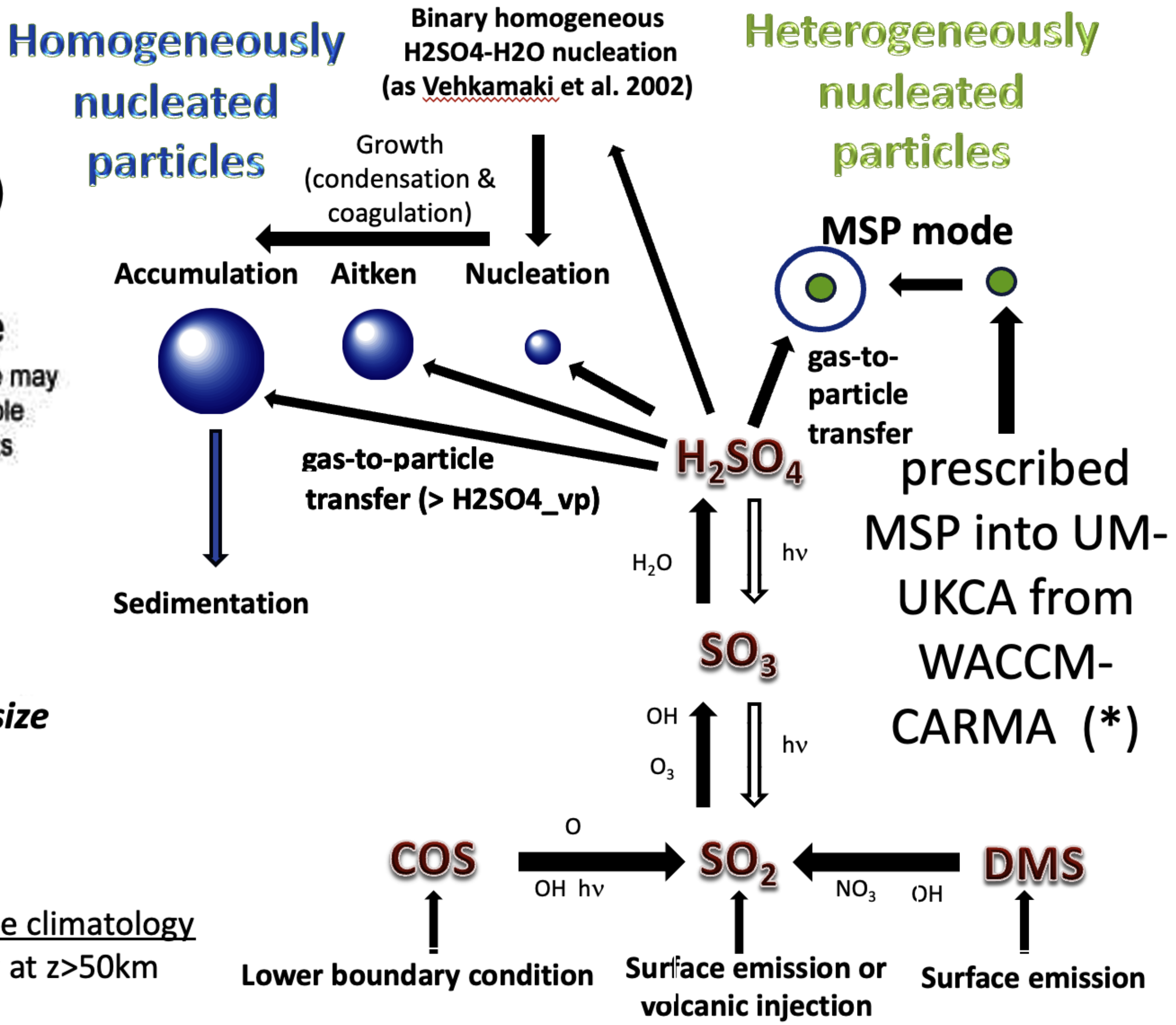

(*) Prescribed Meteoric Smoke Particle climatology
Number & mass mixing ratios of MSP at z>50km from 140km-lid WACCM-CARMA runs (Bardeen et al. , 2008).

Fig 2b. Schematic of UM-UKCA stratospheric sulphur chemistry and coupling to GLOMAP-mode aerosol microphysics (see Dhomse et al., 2014) with whole-atmosphere "Chemistry of Stratosphere & Trosphere" (CheST).

Stratospheric aerosol processes → vertical & meridional variations in particle size

A key aspect is that the aerosol particles that form in the tropics (initially a few nm, but growing to a few 100 nm) remain suspended in the stratospheric air for ~1-3 yrs (so-called "**Tropical Stratospheric Reservoir**")

Stratospheric processes (microphysics & dynamics) → **vertical & meridional variations in particle size**

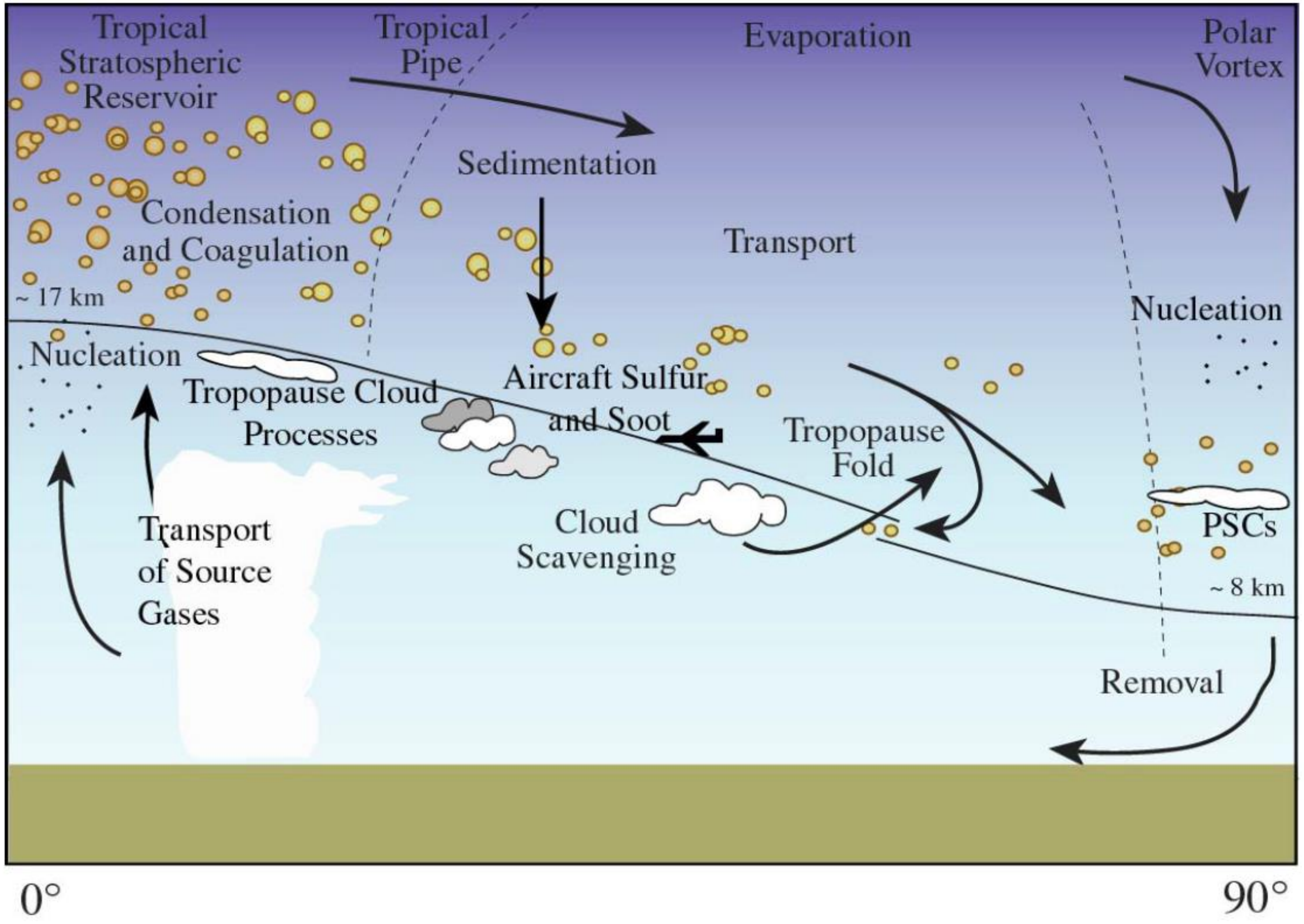

Carslaw & Karcher (2006)
(ch1 of SPARC "ASAP report", 2006; diagram adapted from version in Hamill et al., 1997 BAMS paper)

Stratospheric aerosol processes → vertical & meridional variations in particle size

A key aspect is that the aerosol particles that form in the tropics (initially a few nm, but growing to a few 100 nm) remain suspended in the stratospheric air for ~1-3 yrs (so-called "**Tropical Stratospheric Reservoir**")

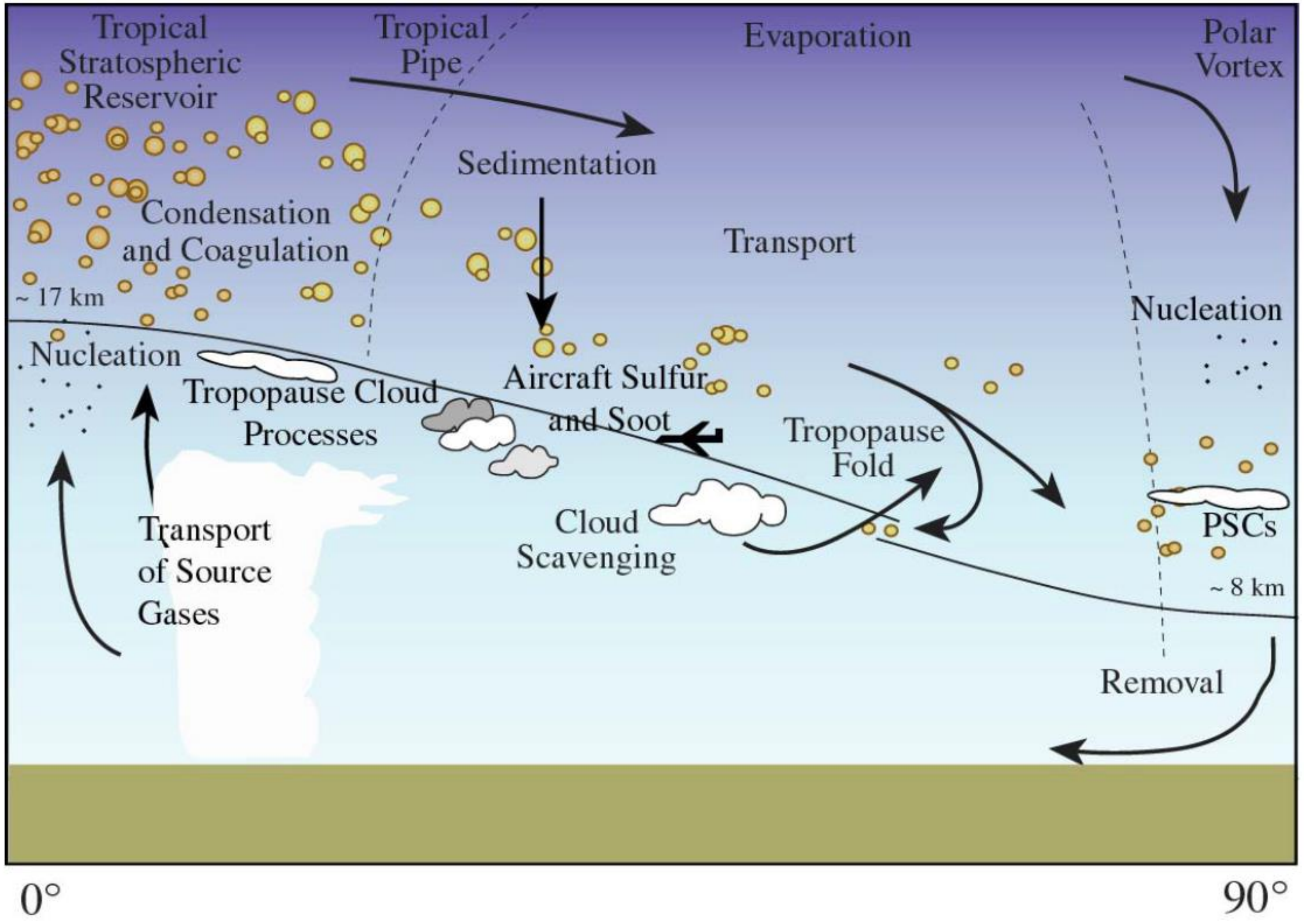

Stratospheric processes (microphysics & dynamics)
→ **vertical & meridional variations in particle size**

After major volcanic eruptions large explosive volcanic **emission of sulphur dioxide** to the stratosphere
→ oxidation, coagulation & condensation **grow the particles to larger sizes**

Carslaw & Karcher (2006)
(ch1 of SPARC "ASAP report", 2006; diagram adapted from version in Hamill et al., 1997 BAMS paper)

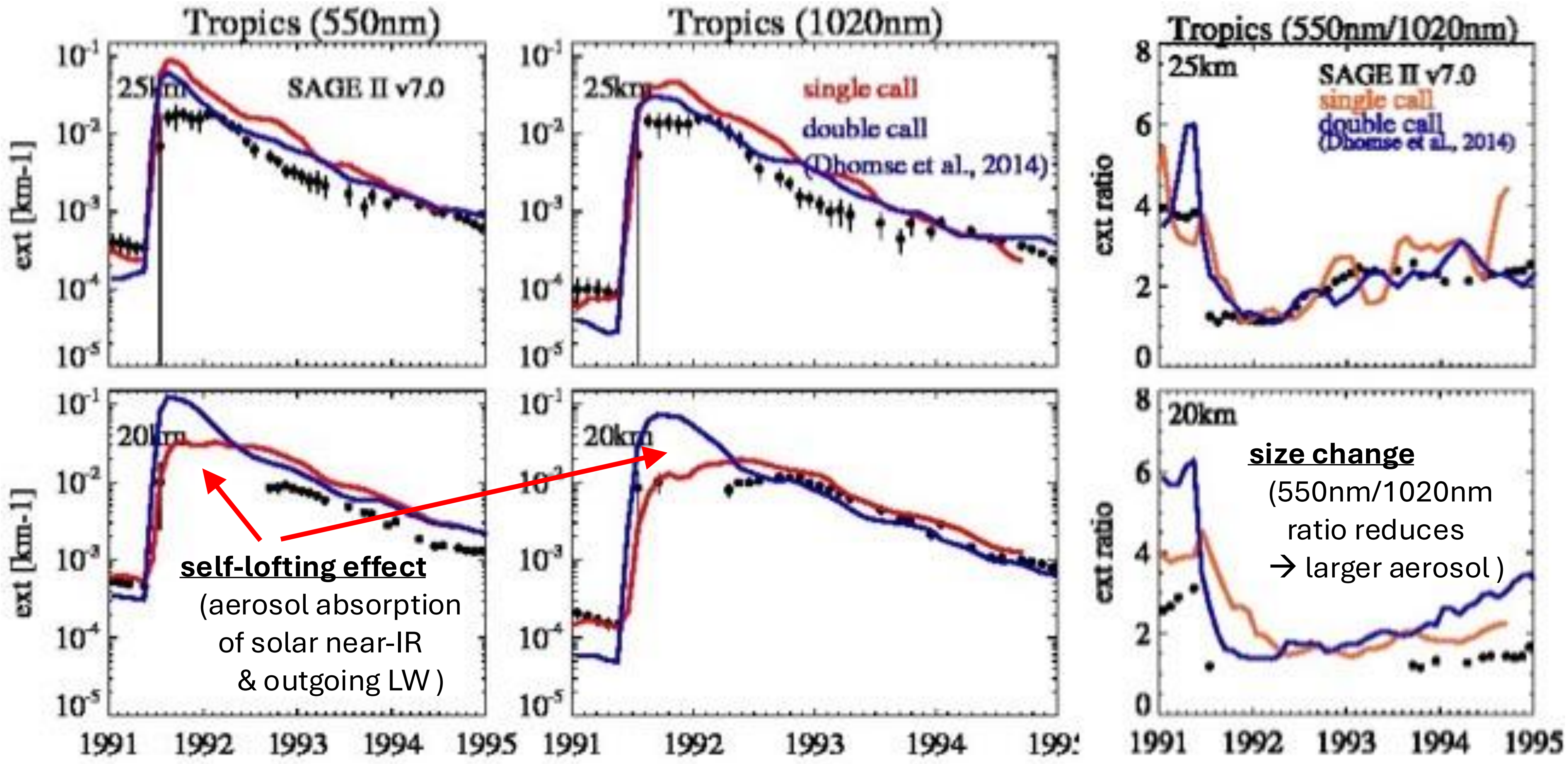

Mann et al. (2015, PAGES)

Comparison UM-UKCA to satellite observations & microphysical aerosol properties (size, SAD) – re-analyse "the first 6 months after"

ERA5-nudged *SO2-only* runs,
aligned to Tonga-MIP protocols

Satellite obs indicate that, in contrast to Pinatubo's absorptive-heating self-lofting, HT-aerosol descended rapidly due to water vapour LW radiative cooling

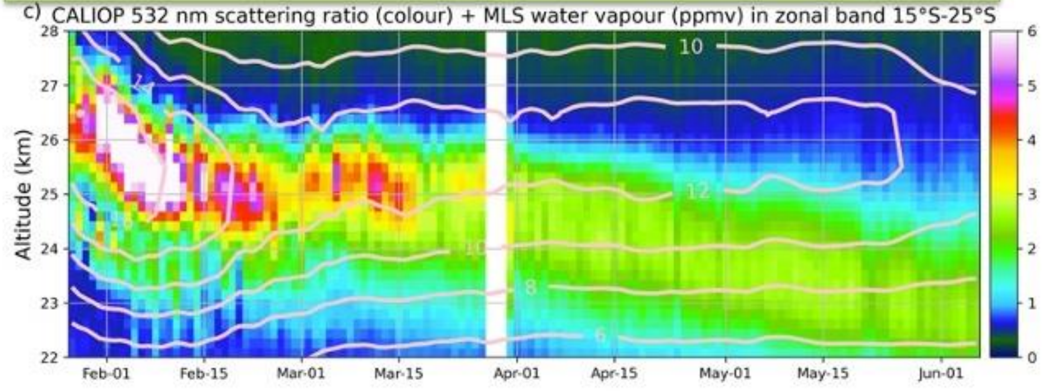

When emitting only SO2, exploring the extent to which can adjust to emit at 23-25km .

These simulations then do not attempt to capture the steep-descent phase, but where the aerosol emerges in mid-February 2022

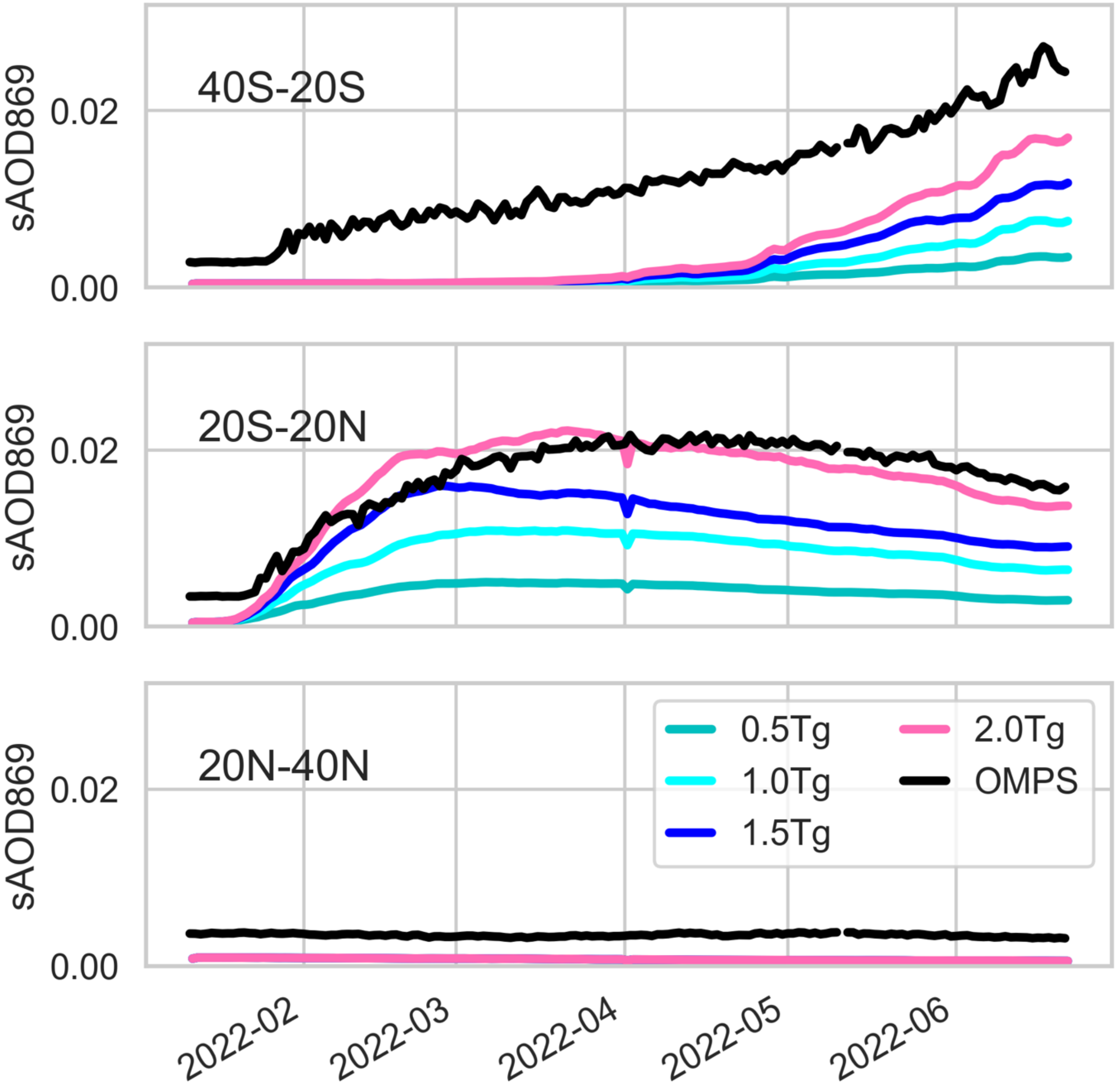

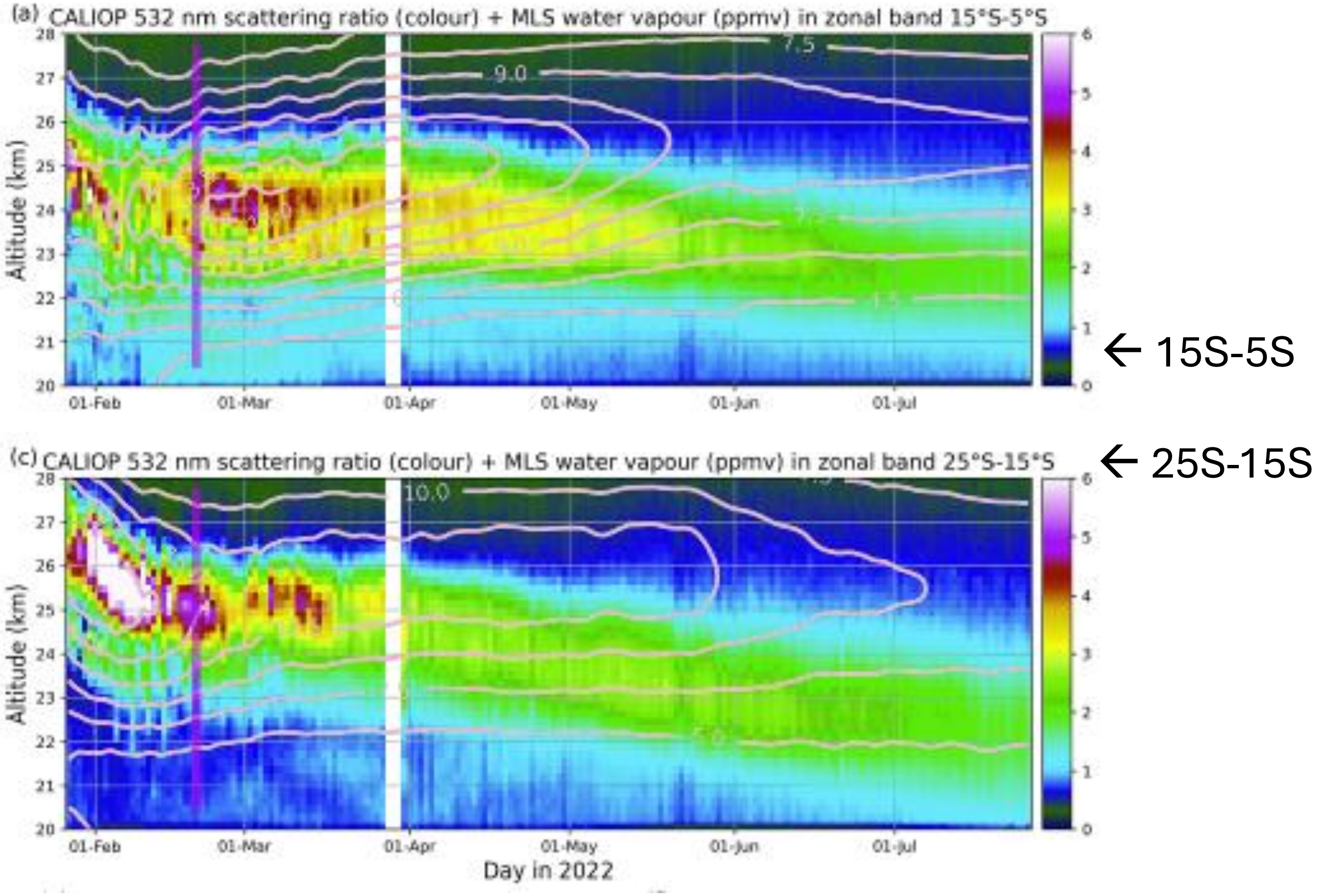

Legras et al. (ACP, 2022)

<u>Separation of volc-aerosol layer from HTHH sWV</u>

→ descent rate provides a potentially important case with **<u>observational constraint for particle size</u>** simulated within the aerosol microphysics models
(combined upwelling & sedimentation)

OMPS-LP observations indicate the Hunga-Tonga aerosol may have penetrated into vortex during August '22 (within the lowermost stratosphere)

But water vapour remained outside the vortex (transported to high latitudes only after vortex breakup).

Wang et al. (JGR, 2023)

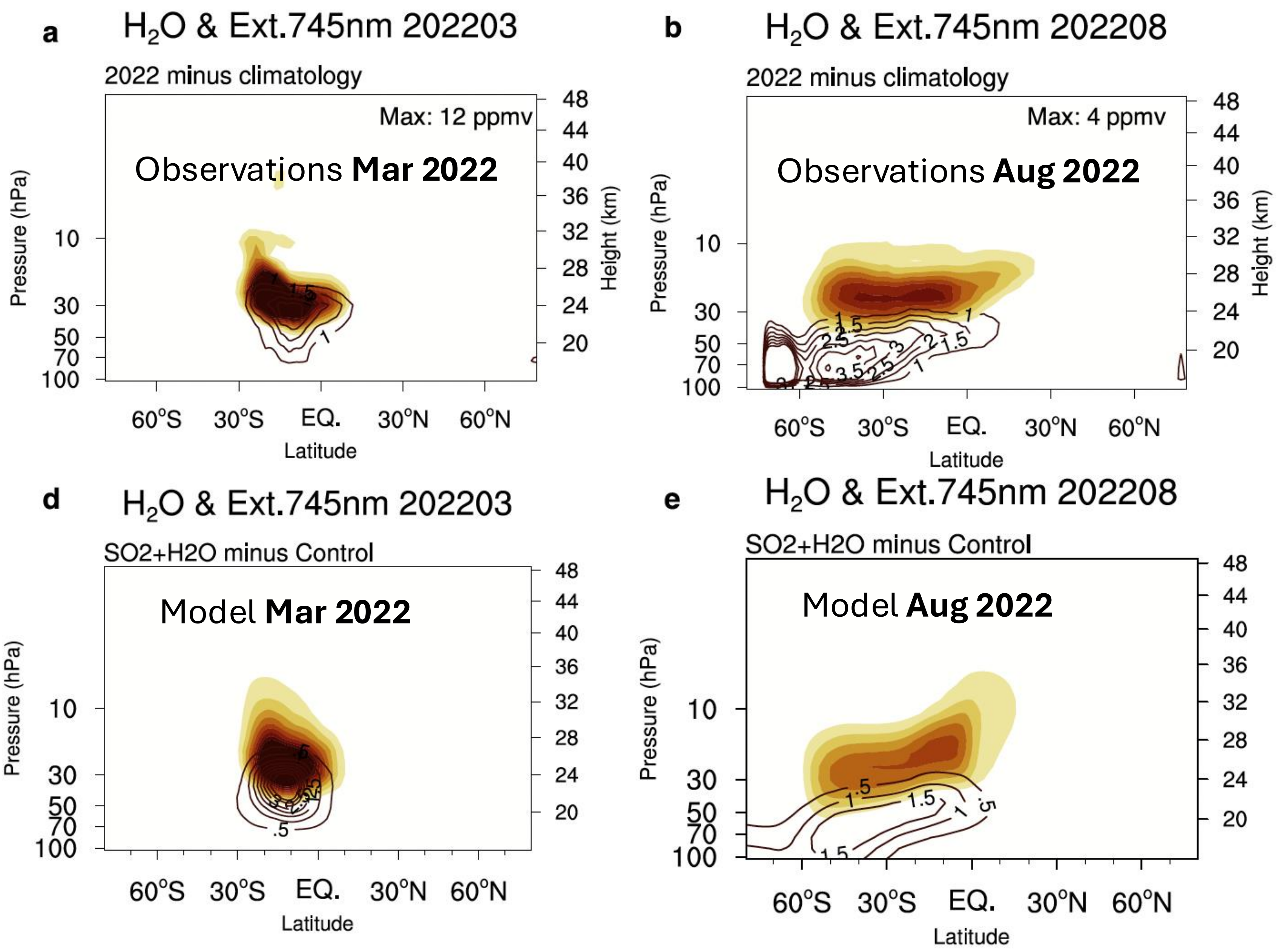

OMPS-LP observations indicate the Hunga-Tonga aerosol may have penetrated into vortex during August ‘22 (within the lowermost stratosphere)

But water vapour remained outside the vortex (transported to high latitudes only after vortex breakup).

Wang et al. (JGR, 2023)

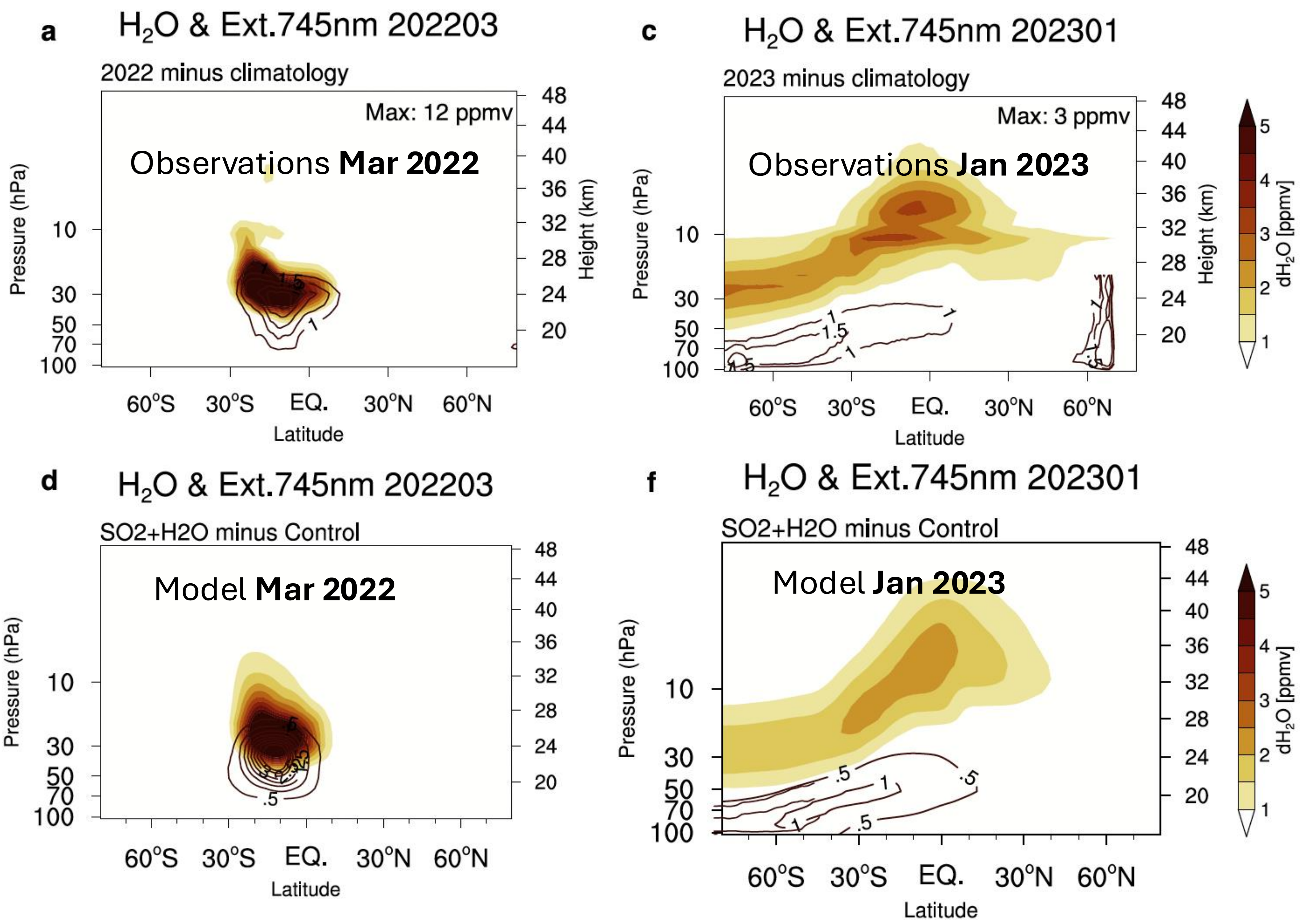

Progression of the Pinatubo aerosol cloud Aug to Sep 1991
(main layer at 20-25km).

Sep '91 Hudson eruption (Chile) formed lower-altitude aerosol layer (10-12km)

Pinatubo aerosol cloud remains northward of 60S (vortex barrier)

Antarctic vortex permeable at lowermost stratosphere, with the SAGE-II measurements showing the lower-altitude layer from Hudson in Antarctic vortex in late-Sep/early-Oct.

Note balloon measurements from McMurdo (Deshler et al., GRL 1992) and from lidar (Adriani et al. 1992) also profiled the Hudson aerosol layer from McMurdo in spring 1991.

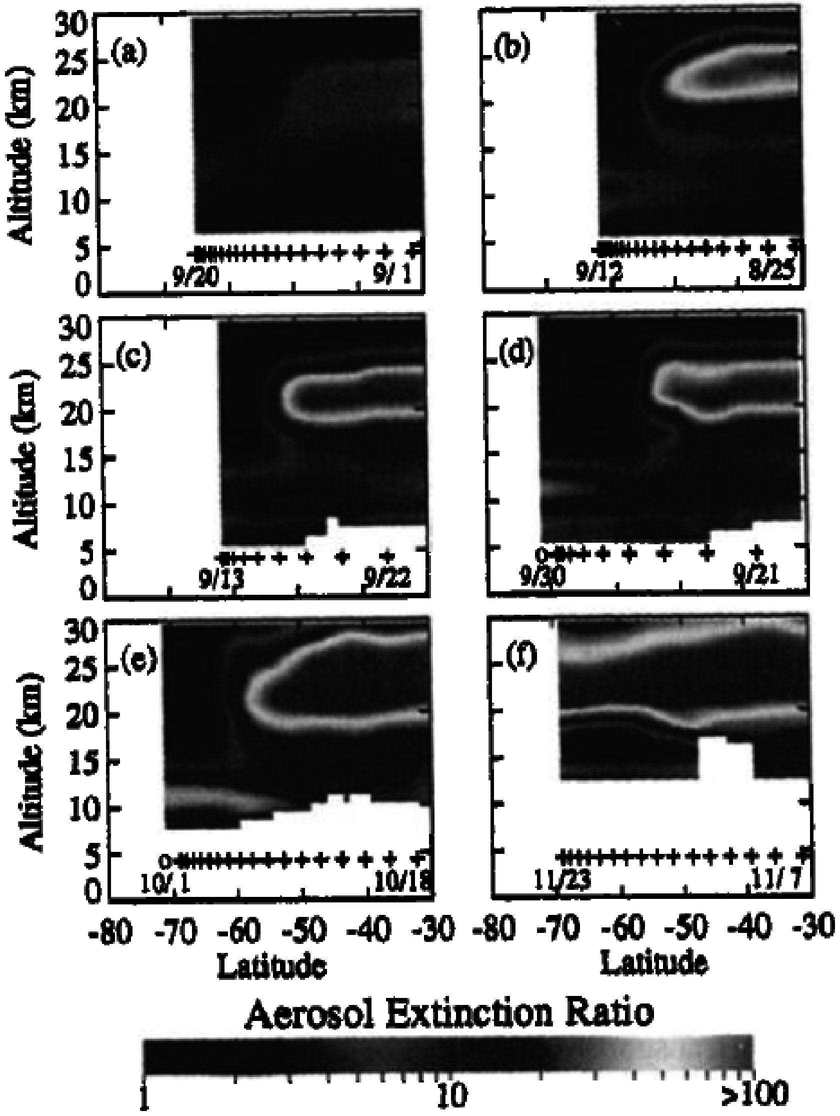

Fig 1. Latitude-altitude median cross sections of SAGE II and SAM II 1-μm aerosol extinction ratio for six periods. The crosses indicate the daily mean latitude of the SAGE II observations and the circles indicate the daily mean latitude of the SAM II observations.

Abstract. At the beginning of the 1991 Austral spring, volcanic aerosols from Mt. Pinatubo and Cerro Hudson were present in the polar stratosphere of the Southern Hemisphere. Satellite observations of aerosol extinction were used to identify and track the movement of these aerosols in the vicinity of the Antarctic vortex during August through November 1991. A layer of mature Mt. Pinatubo aerosols was identified near 21 km and a layer of fresh Cerro Hudson aerosols was identified near 12 km. This altitude separation of the Mt. Pinatubo and Cerro Hudson aerosols was observed throughout the period. Below 15 km, the polar stratosphere was subject to episodes of strong wave activity which transported the Cerro Hudson aerosols poleward and, after the middle of September, they became a persistent feature beneath the vortex. Above 15 km, signatures of Mt. Pinatubo aerosols were observed near the vortex boundary, but significant portions of the vortex interior remained free of any detectable intrusions of Mt. Pinatubo aerosols until the final warming in mid-November.

Pitts & Thomason (GRL, 1993)

Bourassa and Khaykin (2025, in prep)
<u>Chapter 3 of 2025 Hunga report</u>

66.7S (Ground-based lidar)

68S-64S (CALIOP)

82S-65S (CALIOP)

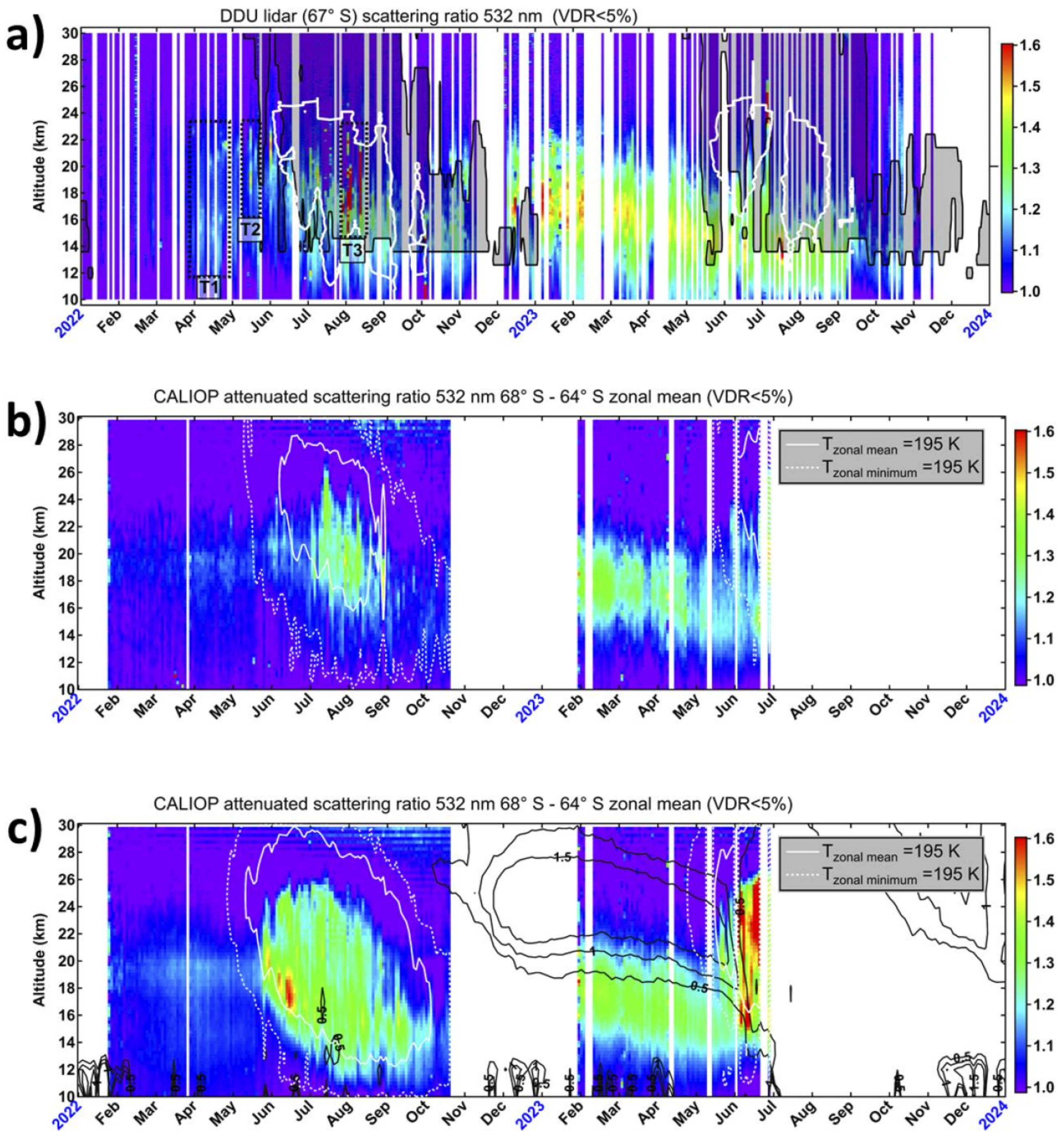

At Dumont D'Urville (DDU) at 66.7^{o}S

CALIOP & DDU data includes only data-pts with depol < 5% (spherical

CALIOP lidar indicates volcanic aerosol *was* transported into polar vortex in Aug-Sep 2022

→ Then potentially consistent with interactive model predictions from Wang et al. (2023)

vortex-avg at 550K

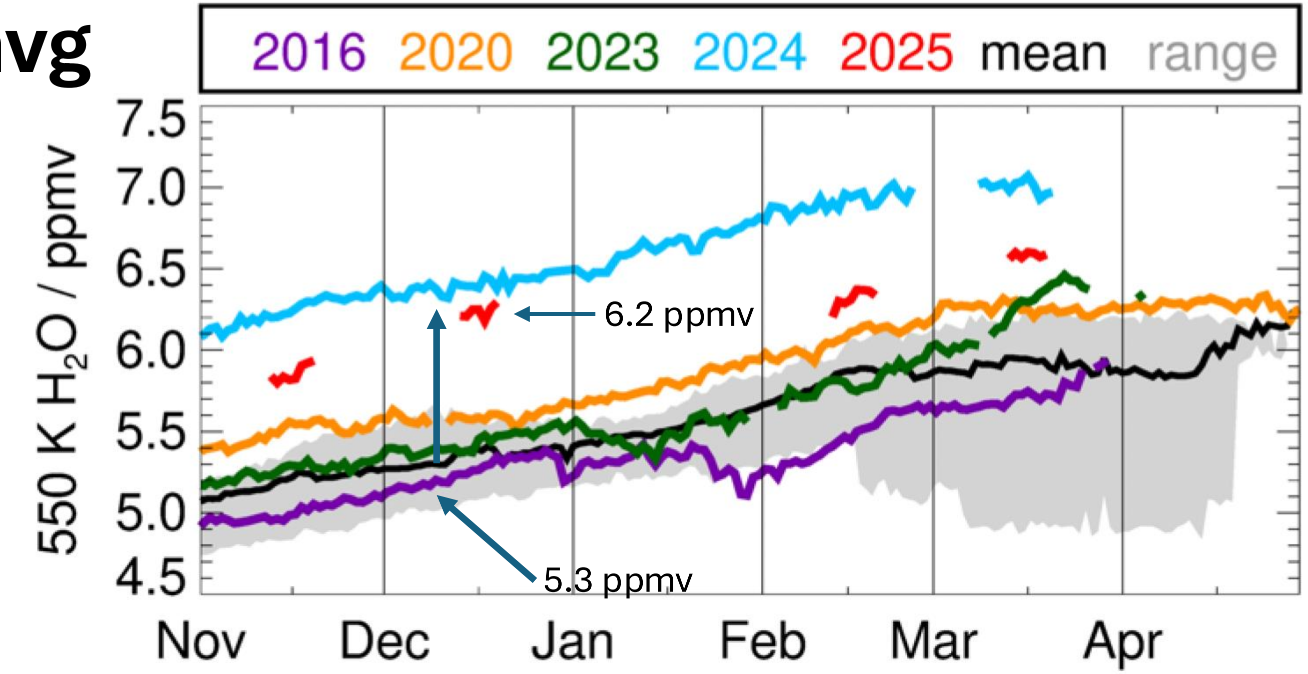

vortex-avg at 480K

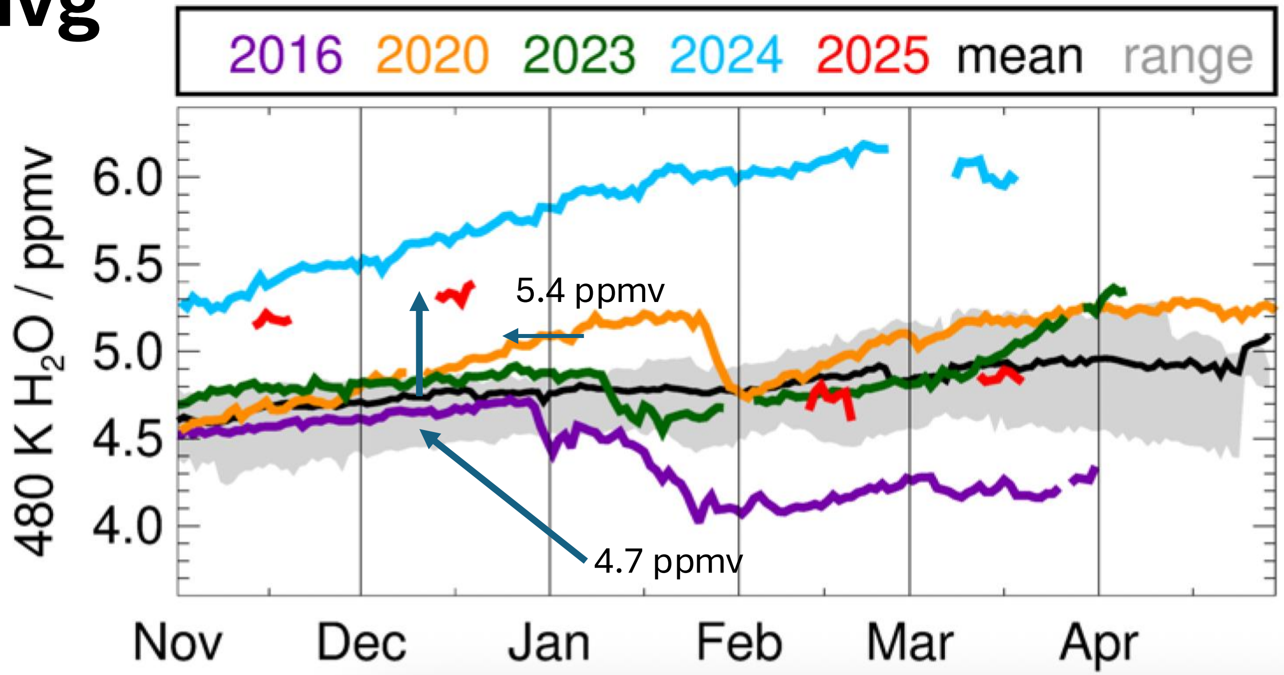

from Michelle Santee
(NASA JPL)

Last 2 Arctic winters Hunga-elevated H_2O

Excess-H2O at 550K
~ 0.9 ppmv in mid-Dec24
(on vortex-avg, 6.2 c.f. 5.3)
(anomaly compared to mean [black])

(increased from ~0.5 ppmv in Nov24)

Excess-H2O at 480K
~ 0.7 ppmv in mid-Dec24
(on vortex-avg, 5.4 c.f. 4.7)
(anomaly compared to mean [black])

(about the same as ~0.7 ppmv in Nov24)

Last 2 Arctic winters Hunga-elevated H_2O

vortex-avg at 750K

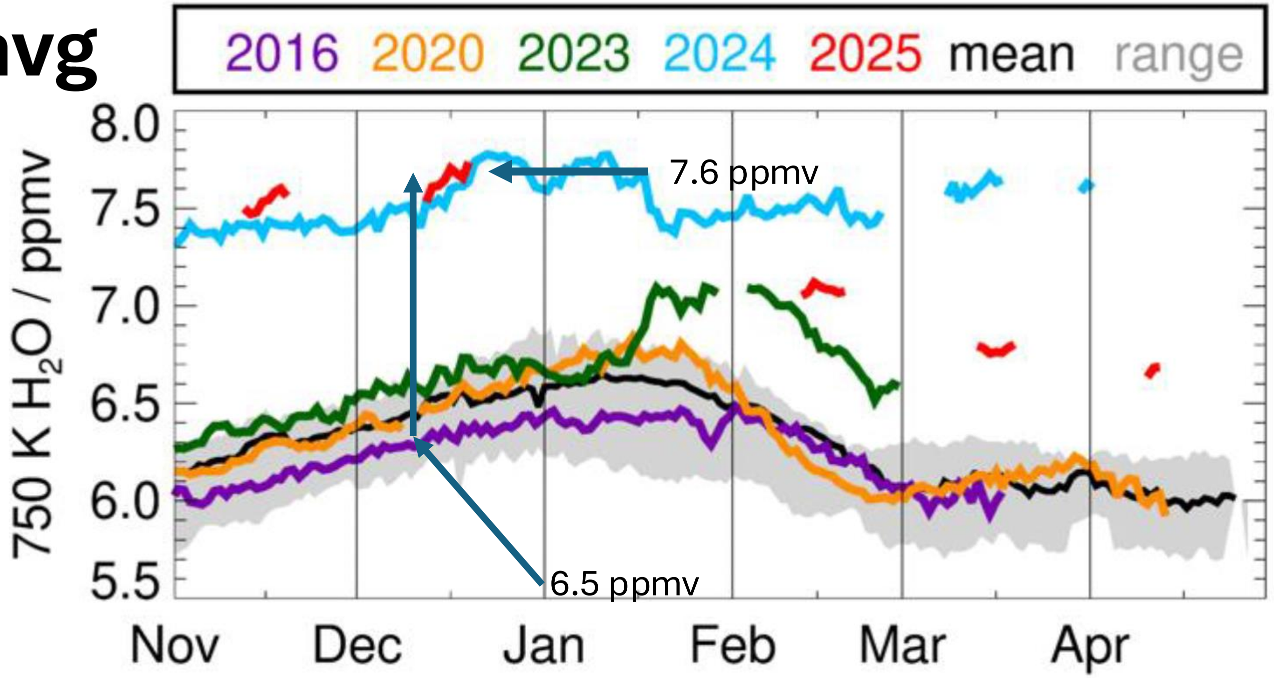

Excess-H2O at 750K ~ 1.1 ppmv in mid-Dec24

(on vortex-avg, 7.6 c.f. 6.5)

(anomaly compared to mean [black])

(similar enhancement ~1.1 ppmv in Nov24)

vortex-avg at 660K

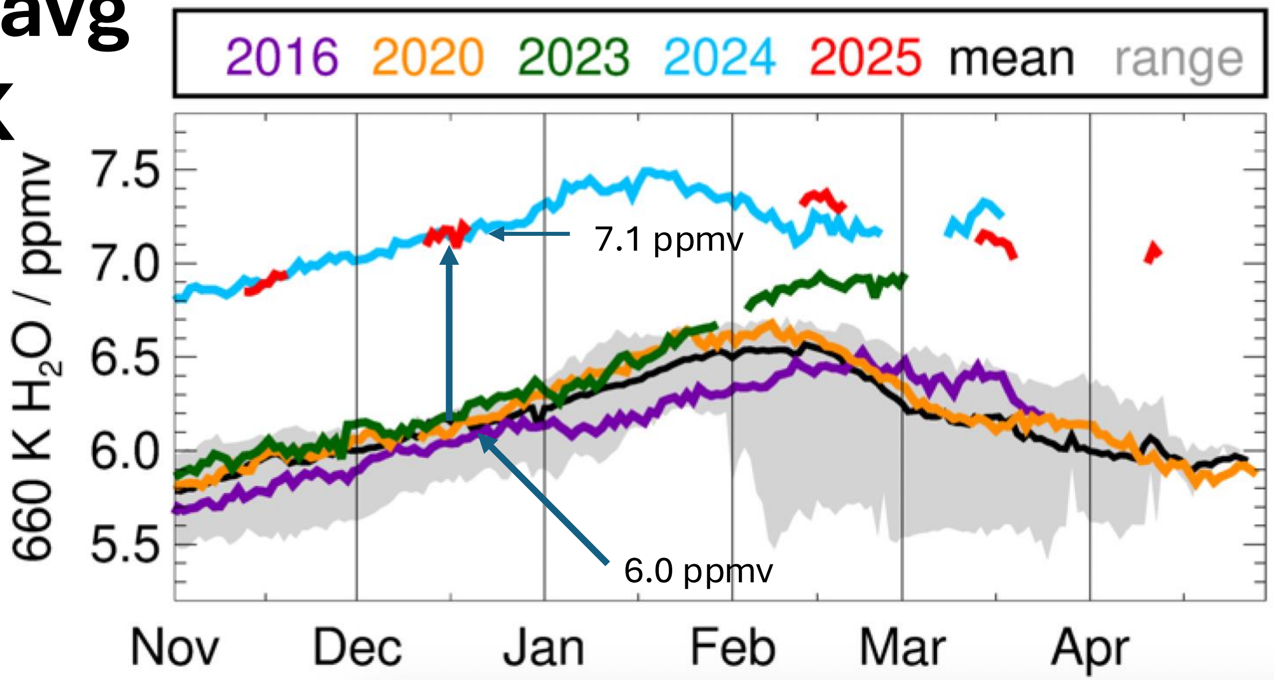

Excess-H2O at 660K ~ 1.1 ppmv in mid-Dec24

(on vortex-avg, 7.1 c.f. 6.0)

(anomaly compared to mean [black])

(and similar enhancement ~1.1 ppmv in Nov24)

from Michelle Santee (NASA JPL)

Atmos. Chem. Phys., 9, 6109–6118, 2009
www.atmos-chem-phys.net/9/6109/2009/

Atmospheric Chemistry and Physics

The climatic effects of the direct injection of water vapour into the stratosphere by large volcanic eruptions

M. M. Joshi[1] **and G. S. Jones**[2]

[1]NCAS Climate, University of Reading, UK
[2]Hadley Centre for Climate Change, Met Office, UK

Received: 20 January 2009 – Published in Atmos. Chem. Phys. Discuss.: 2 March 2009
Revised: 7 August 2009 – Accepted: 10 August 2009 – Published: 25 August 2009

Joshi and Jones (2009, ACP) presented the possibility that **explosive eruptions** can also cause a **positive radiative forcing from increased stratospheric water vapour**

→ to have **potentially offset a proportion of the** dominant **volcanic aerosol surface cooling** after **1883 Krakatau**

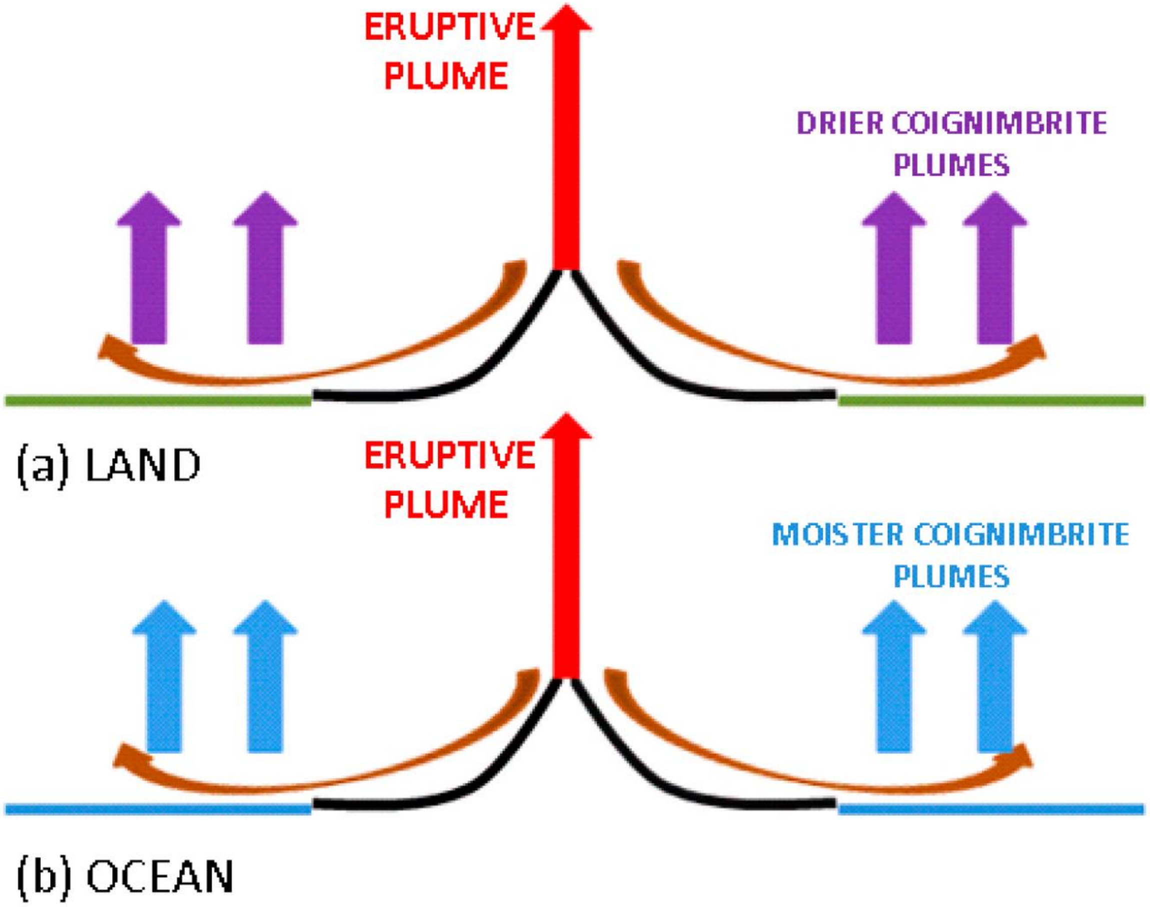

Phreatomagmatic activity can also result from magma interaction with external water in subterranean aquifer systems. Two typical examples include the Ukinrek Maars explosions in 1977 and the last two phases of the Vesuvius eruption in AD 79. In the case of Ukinrek Maars, Self *et al.* (1980) have suggested that the craters that were observed following the explosions were the result of "the collapse of crater and conduit walls, and the blasting-out of debris by phreatomagmatic explosions when the rising magma contacted groundwater beneath the regional water table and a local perched aquifer". Following the initial phase of the AD 79 Vesuvius eruption Sheridan *et al.* (1981) have suggested that cavitation of the roof and walls resulted in rupture of the metamorphic encasement surrounding the conduit and led to interaction of the magma with the regional hydrologic system. They further conjecture that "because the magma level within the emptying chamber was below the principal aquifer . . . an abundant source of water was available . . . when the venting pressure dropped below the hydrostatic head".

Magma–water interactions can also take place after silicic magma has been fragmented and discharged from a vent (Walker 1979). Many ignimbrite-forming volcanic centres are near large water bodies or the sea. During explosive eruptions hot pyroclastic flows can be discharged into water (e.g. Cas and Wright 1991). For example, during the 1883 eruptions of Krakatoa volcano in Indonesia, voluminous dacite pyroclastic flows were discharged into the Sunda Straits (Self and Rampino 1981; Sigurdsson *et al.* 1991). Parts of the flow were emplaced subaqueously at high temperature (Mandeville *et al.* 1994), whereas less dense and more turbulent portions continued over the sea surface for distances up to 80 km (Carey *et al.* 1996). The phreatomagmatic interaction of the flows with seawater generated a moisture-rich co-ignimbrite plume and widespread fallout of mud rain. Walker (1979) proposed similar processes of ash plume generation for pyroclastic flows entering the sea in the Taupo Volcanic Zone.

Current modelling efforts suggest that the efficiency of magma–water interaction is controlled by the mass of water mixing into the eruption products, with values of about 0.35 yielding the most intense interactions (Wohletz 1983; Wohletz and Heiken 1992). The following sections discuss the explosive energy and fragmentation that result from magma–water interaction and the properties of erupting water–magma mixtures.

8.5.1 Explosive Energy and Fragmentation

If external water from the sea or a lake mixes with erupting magma, or if the conduit intersects a shallow aquifer, then there may be a very intense interaction which produces a highly fragmented mixture (Walker and Croasdale 1972; Walker 1973; Self and Sparks 1978). The energy driving this fragmentation is derived from the heating and expansion of the water as it comes into contact with the very hot magma. For example, if liquid water is heated to 1200 °C at a fixed volume then the pressure increases to about 500 MPa Thus explosive activity can be much more intense but often characterized by large fluctuations, as typified by the Surtsey example above. Therefore, the total power output from such eruptions is no larger than magmatic eruptions, since in both cases the thermal energy of the magma is the main source of energy.

The rapid chilling, contraction and fracture of the magma when it interacts with the external water can produce blocky ash fragments with planar surfaces (Self and Sparks 1978; Heiken and Wohletz 1985). In some situations, the fragmentation process may be

Magma–water interactions can also take place after silicic magma has been fragmented and discharged from a vent (Walker 1979). Many ignimbrite-forming volcanic centres are near large water bodies or the sea. During explosive eruptions hot pyroclastic flows can be discharged into water (e.g. Cas and Wright 1991). For example, during the 1883 eruptions of Krakatoa volcano in Indonesia, voluminous dacite pyroclastic flows were discharged into the Sunda Straits (Self and Rampino 1981; Sigurdsson *et al.* 1991). Parts of the flow were emplaced subaqueously at high temperature (Mandeville *et al.* 1994), whereas less dense and more turbulent portions continued over the sea surface for distances up to 80 km (Carey *et al.* 1996). The phreatomagmatic interaction of the flows with seawater generated a moisture-rich co-ignimbrite plume and widespread fallout of mud rain. Walker (1979) proposed similar processes of ash plume generation for pyroclastic flows entering the sea in the Taupo Volcanic Zone.

Sparks et al. (1997) text book "Volcanic Plumes"

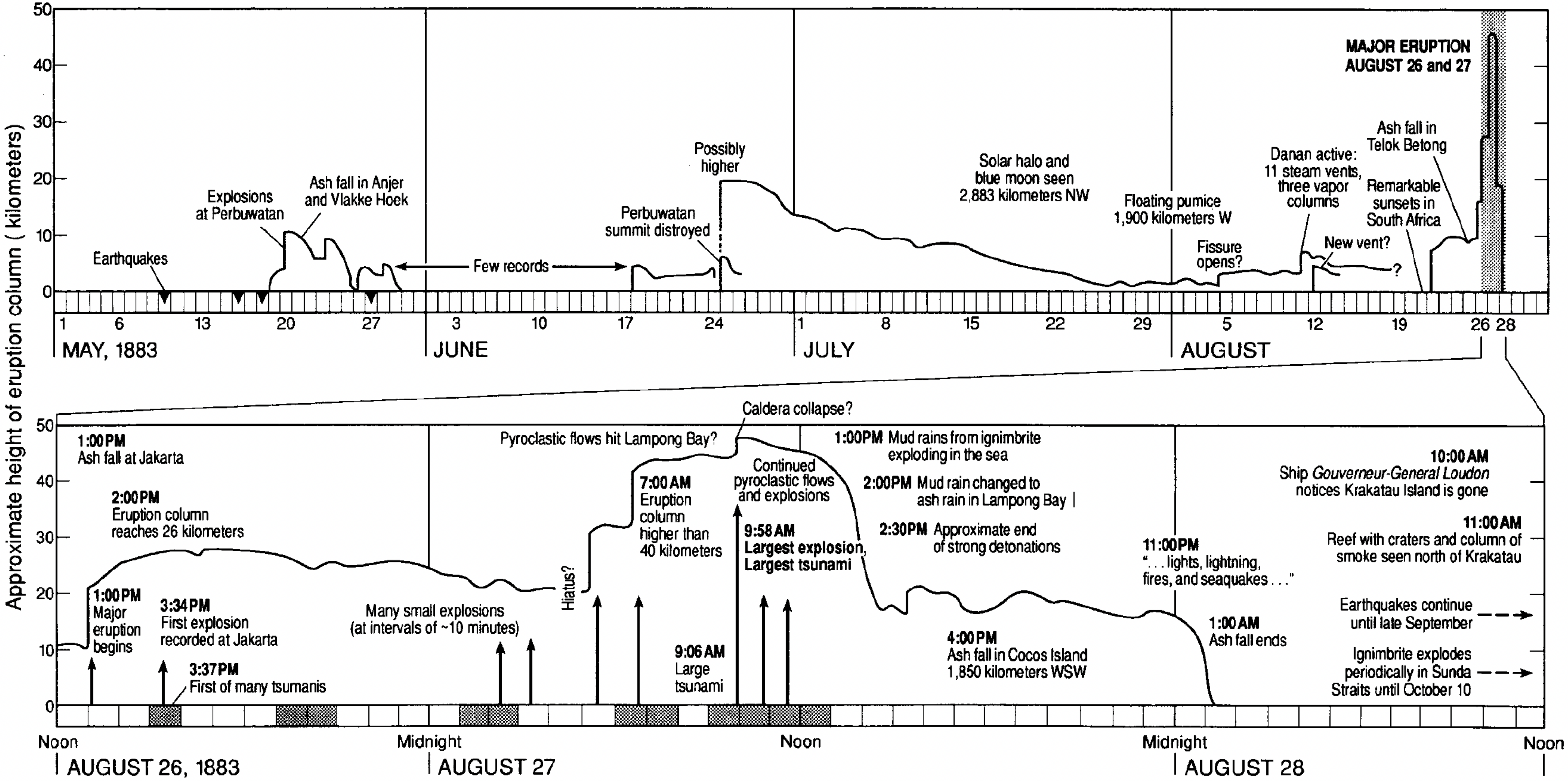

Self (1992, Geojournal)

→ Krakatau eruption chronology

Main 10am Aug 27th = a sea-water explosion → ignimbrite plume

→ direct H_2O injection to ~40km

Spread of the Krakatoa Volcanic Dust Cloud as Related to the High-Level Circulation

H. WEXLER

U. S. Weather Bureau, Washington, D. C.

ABSTRACT

The spread of volcanic dust from the explosion of Krakatoa is described. An explanation of the initial rapid lateral spread poleward in the Northern Hemisphere, the much slower spread in the second month, and the accelerated spread in the third and fourth months is attempted in terms of the normal monthly circulations at 19 km.

On August 27, 1883, following several months of minor explosions, the volcano on the Island of Krakatoa (Sunda Strait, between Sumatra and Java, 6° 9′ S, 105° 22′ E) blew up and ejected into the atmosphere an estimated 13 cubic miles of lava, ash, and mud. About one-third of the material fell within 30 miles, covering some places 25 miles distant with deposits to a depth of one foot. Another third, composed of fine dust, fell within 2,000 miles, while the remainder, consisting mostly of very fine pumiceous bubble plates settled out slowly from the atmosphere for several years and produced unusual optical effects, such as the remarkable twilight glows, colored suns and moons, and the "Bishop's Ring."

A committee appointed by the Royal Society of London studied various aspects of the explosion and summarized their findings in the classic "Eruption of Krakatoa" [6]. From their analysis of hundreds of observations they were able to plot roughly the spread of the volcanic cloud in the northern and southern hemispheres. One of their results showed that it took approximately three months for the cloud to travel to western Europe in concentrations large and persistent enough to produce the unusual and prolonged optical effects observed. It was pointed out in a previous paper by the present writer [7] that coincident with the appearance of the optical phenomena in western Europe during the last

Wexler et al. (1951, BAMS)

Spread of the Krakatoa Volcanic Dust Cloud as Related to the High-Level Circulation

Here are the known facts as to the spread of the cloud as deduced by optical observations and summarized from material presented in "Eruption of Krakatoa" [6].

1. Apart from off-shoots towards Japan and South Africa immediately after the explosion, the main body of the cloud moved from east to west at an average speed of 73 miles per hour, completing at least two circuits of the earth in equatorial latitudes.

2. The cloud in making these circuits passed over most places in three or four days which, combined with the speed of travel of the leading edge, indicates that the cloud was drawn out to a length of 5,000 to 7,000 miles, presumably by the vertical shear in the equatorial easterlies.

3. Excluding sporadic twilight glows, due probably to small, broken-off masses of the cloud, the northern extreme limit observed at the end of the first circuit (Sept. 9) was 22° N (Honolulu) and the southern extreme limit 33° S at Santiago, Chile. The average limits were 16° N and 22° S.

4. At the end of the second circuit (Sept. 22) the average cloud limits extended roughly from 24° N to 40° S.

5. North of latitude 30° N there was no further indication of spread of the cloud from east to west. In October when the cloud material had reached 30° N there were fewer accounts of its having travelled to new places than before or after that date, and during that month it spread only slightly in latitude.

6. The twilight glows spread gradually northward and southward, but up to about November 23 the glows seen north of about 32° to 36° N were for the most part sporadic, apparently caused by detached portions from the main cloud.

7. On November 23 a remarkable movement took place in such a manner that by November 27 the twilight glows were generally observed over the United States and Europe; they are believed to have spread to these regions from the mid-Pacific and mid-Atlantic oceans respectively.

8. After December 1883 it was not possible to follow the main cloud as a distinct entity.

Wexler et al. (1951, BAMS)

Spread of the Krakatoa Volcanic Dust Cloud as Related to the High-Level Circulation

H. Wexler

U. S. Weather Bureau, Washington, D. C.

Abstract

The spread of volcanic dust from the explosion of Krakatoa is described. An explanation of the initial rapid lateral spread poleward in the Northern Hemisphere, the much slower spread in the second month, and the accelerated spread in the third and fourth months is attempted in terms of the normal monthly circulations at 19 km.

surface.

In absence of current upper air charts in 1883 the proposed explanation will be based on the normal monthly upper air charts for the Northern Hemisphere [1]. The August, September, October, and November normal charts at 19 km (the highest level available) will be used as a guide in explaining the observed travel of the northern hemispheric portion of the main cloud whose top was computed from optical effects and rate-of-fall formulae [4] to have decreased in height from 32 km in August 1883 to 17 km in January 1884. An earlier attempt was made by C. E. P. Brooks [2] to relate the motion of the Krakatoa cloud in the Northern Hemisphere with a much lower level, namely the average cirrus motion (8 to 11 km) during the months of October to December.

explaining the observed travel of the northern hemispheric portion of the main cloud whose top was computed from optical effects and rate-of-fall formulae [4] to have decreased in height from 32 km in August 1883 to 17 km in January 1884. An

[2] Brooks, C. E. P., The movement of Volcanic Ash over the Globe, *Met. Mag.*, 67, 81, 1932.
[3] Newell, H. E., Jr., Upper Air Research by Rockets, *Trans. Am. Geophy. Union*, 31, 1, pp. 25–33, 1950.
[4] Pernter, J. M., Der Krakatau-Ausbruch und seine Folge-Erscheinungen, *Met. Zeit.*, 6, pp. 329, 409, 447, 1889.

Wexler et al. (1951, BAMS)

Pernter et al. (1889, article in Meteorologische Zeitschrift)

page 456

Dass die Ursache der Purpurlichter und der Dämmerung überhaupt in den in der Atmosphäre schwebenden Staubtheilchen oder Kondensations-Produkten des Wassers liegt, ist bekannt. Je höher diese Trübungen in die Atmosphäre hinaufreichen, desto länger währt die Dämmerung, bezw. die Purpurlichter. Die Dauer dieser Erscheinungen und die Höhe der höchsten lichtzerstreuenden Schichten hängt nach einem einfachen Gesetze zusammen, so dass man aus ersterer die letztere berechnen kann. Es lag nahe, aus der Dauer der ungewöhnlichen Dämmerungen die Höhe jenes Dunstnebels zu berechnen, der gleichzeitig mit denselben beobachtet wurde und der die offenkundige Ursache sowohl des grösseren Glanzes als der längeren Dauer der Purpurlichter war. Die Art und Weise dieser Berechnung ist nichts

ch auf O. Jesse's
kann natürlich
hnung benützen,
die Dunstnebel-
te als Reflex des
Reflexion an dem
ald bediente sich

Purpurlichtes

$$h = R \operatorname{tng} \frac{\alpha_1}{2} \operatorname{tng} \frac{\alpha_1}{4}$$

b) Aus der Zeit des

It is well known that **the cause of the purple lights and of twilight in general lies in the dust particles** or condensation products of water floating in the atmosphere.

The higher these clouds reach into the atmosphere, **the longer the twilight or the purple lights last**.

The duration of these phenomena and the height of the highest light-destroying layers are related by a simple law, so that the latter can be calculated from the former.

It was obvious to **calculate from the time of the unusual twilights the height of the haze** that was observed at the same time and which was the obvious cause of both the greater brightness and the longer duration of the purple lights.

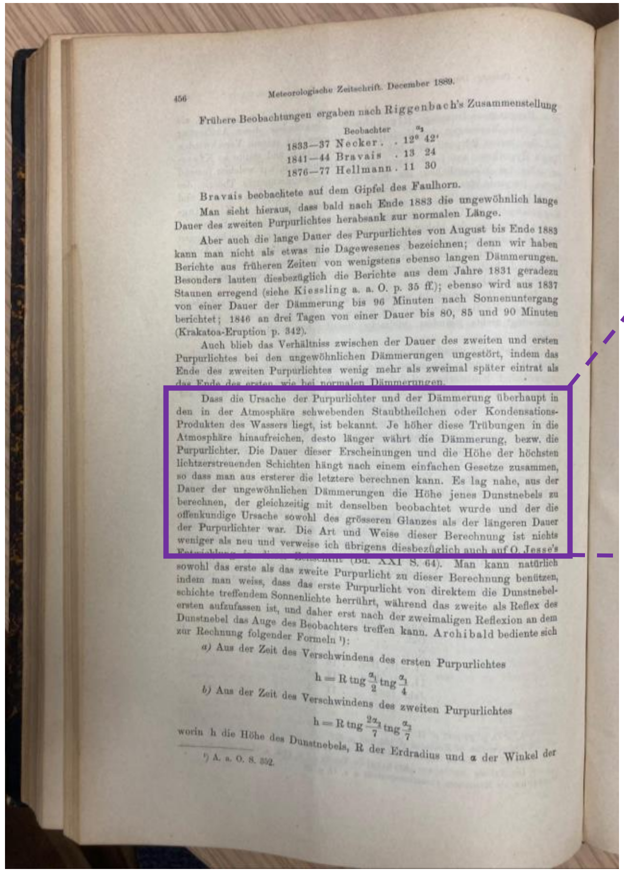
456 Meteorologische Zeitschrift. December 1889.

Frühere Beobachtungen ergaben nach Riggenbach's Zusammenstellung

	Beobachter	α_1
1833—37	Necker. .	12° 42′
1841—44	Bravais .	13 24
1876—77	Hellmann.	11 30

Bravais beobachtete auf dem Gipfel des Faulhorn.

Man sieht hieraus, dass bald nach Ende 1883 die ungewöhnlich lange Dauer des zweiten Purpurlichtes herabsank zur normalen Länge.

Aber auch die lange Dauer des Purpurlichtes von August bis Ende 1883 kann man nicht als etwas nie Dagewesenes bezeichnen; denn wir haben Berichte aus früheren Zeiten von wenigstens ebenso langen Dämmerungen. Besonders lauten diesbezüglich die Berichte aus dem Jahre 1831 geradezu Staunen erregend (siehe Kiessling a. a. O. p. 35 ff.); ebenso wird aus 1837 von einer Dauer der Dämmerung bis 96 Minuten nach Sonnenuntergang berichtet; 1846 an drei Tagen von einer Dauer bis 80, 85 und 90 Minuten (Krakatoa-Eruption p. 342).

Auch blieb das Verhältniss zwischen der Dauer des zweiten und ersten Purpurlichtes bei den ungewöhnlichen Dämmerungen ungestört, indem das Ende des zweiten Purpurlichtes wenig mehr als zweimal später eintrat als das Ende des ersten, wie bei normalen Dämmerungen.

Dass die Ursache der Purpurlichter und der Dämmerung überhaupt in den in der Atmosphäre schwebenden Staubtheilchen oder Kondensations-Produkten des Wassers liegt, ist bekannt. Je höher diese Trübungen in die Atmosphäre hinaufreichen, desto länger währt die Dämmerung, bezw. die Purpurlichter. Die Dauer dieser Erscheinungen und die Höhe der höchsten lichtzerstreuenden Schichten hängt nach einem einfachen Gesetze zusammen, so dass man aus ersterer die letztere berechnen kann. Es lag nahe, aus der Dauer der ungewöhnlichen Dämmerungen die Höhe jenes Dunstnebels zu berechnen, der gleichzeitig mit denselben beobachtet wurde und der die offenkundige Ursache sowohl des grösseren Glanzes als der längeren Dauer der Purpurlichter war. Die Art und Weise dieser Berechnung ist nichts weniger als neu und verweise ich übrigens diesbezüglich auch auf O. Jesse's [illegible] (Bd. XXI S. 64). Man kann natürlich sowohl das erste als das zweite Purpurlicht zu dieser Berechnung benützen, indem man weiss, dass das erste Purpurlicht von direktem die Dunstnebelschichte treffendem Sonnenlichte herrührt, während das zweite als Reflex des ersten aufzufassen ist, und daher erst nach der zweimaligen Reflexion an dem Dunstnebel das Auge des Beobachters treffen kann. Archibald bediente sich zur Rechnung folgender Formeln [1]:

a) Aus der Zeit des Verschwindens des ersten Purpurlichtes

$$h = R \operatorname{tng} \frac{\alpha_1}{2} \operatorname{tng} \frac{\alpha_1}{4}$$

b) Aus der Zeit des Verschwindens des zweiten Purpurlichtes

$$h = R \operatorname{tng} \frac{2\alpha_2}{7} \operatorname{tng} \frac{\alpha_2}{7}$$

worin h die Höhe des Dunstnebels, R der Erdradius und α der Winkel der

[1] A. a. O. S. 352.

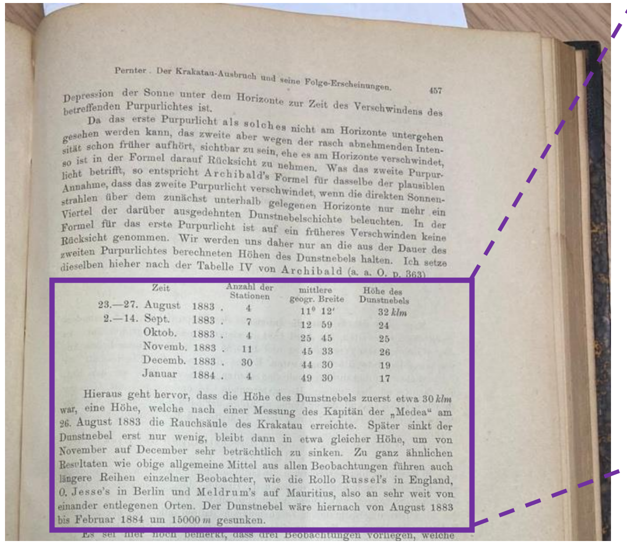
Pernter. Der Krakatau-Ausbruch und seine Folge-Erscheinungen. 457

Depression der Sonne unter dem Horizonte zur Zeit des Verschwindens des betreffenden Purpurlichtes ist.

Da das erste Purpurlicht als solches nicht am Horizonte untergehen gesehen werden kann, das zweite aber wegen der rasch abnehmenden Intensität schon früher aufhört, sichtbar zu sein, ehe es am Horizonte verschwindet, so ist in der Formel darauf Rücksicht zu nehmen. Was das zweite Purpurlicht betrifft, so entspricht Archibald's Formel für dasselbe der plausiblen Annahme, dass das zweite Purpurlicht verschwindet, wenn die direkten Sonnenstrahlen über dem zunächst unterhalb gelegenen Horizonte nur mehr ein Viertel der darüber ausgedehnten Dunstnebelschichte beleuchten. In der Formel für das erste Purpurlicht ist auf ein früheres Verschwinden keine Rücksicht genommen. Wir werden uns daher nur an die aus der Dauer des zweiten Purpurlichtes berechneten Höhen des Dunstnebels halten. Ich setze dieselben hieher nach der Tabelle IV von Archibald (a. a. O. p. 363).

Zeit			Anzahl der Stationen	mittlere geogr. Breite	Höhe des Dunstnebels
23.—27.	August	1883 .	4	11° 12′	32 *klm*
2.—14.	Sept.	1883 .	7	12 59	24
	Oktob.	1883 .	4	25 45	25
	Novemb.	1883 .	11	45 33	26
	Decemb.	1883 .	30	44 30	19
	Januar	1884 .	4	49 30	17

Hieraus geht hervor, dass die Höhe des Dunstnebels zuerst etwa 30 *klm* war, eine Höhe, welche nach einer Messung des Kapitän der „Medea" am 26. August 1883 die Rauchsäule des Krakatau erreichte. Später sinkt der Dunstnebel erst nur wenig, bleibt dann in etwa gleicher Höhe, um von November auf December sehr beträchtlich zu sinken. Zu ganz ähnlichen Resultaten wie obige allgemeine Mittel aus allen Beobachtungen führen auch längere Reihen einzelner Beobachter, wie die Rollo Russel's in England, O. Jesse's in Berlin und Meldrum's auf Mauritius, also an sehr weit von einander entlegenen Orten. Der Dunstnebel wäre hiernach von August 1883 bis Februar 1884 um 15000 *m* gesunken.

Es sei hier noch bemerkt, dass drei Beobachtungen vorliegen, welche

page 456

It is well known that **the cause of the purple lights and of twilight in general lies in the dust particles** or condensation products of water floating in the atmosphere.

The higher these clouds reach into the atmosphere, **the longer the twilight or the purple lights last**.

The duration of these phenomena and the height of the highest light-destroying layers are related by a simple law, so that the latter can be calculated from the former.

It was obvious to **calculate from the time of the unusual twilights the height of the haze** that was observed at the same time and which was the obvious cause of both the greater brightness and the longer duration of the purple lights.

...

page 457

Time	no. of stations	middle geographical latitude	height of the haze
Aug 23-27, 1883.	4	11 12	32 km
Sept 2-14 1883.	7	12 59	24 km
October 1883.	4	25 45	25 km
November 1883	11	45 33	26 km
December 1883	30	44 30	19 km
January 1884	4	49 30	17 km

From this it can be seen that the height of the haze was at first about 30 km, a height which, according to a measurement by the captain of the Medea on August 2nd, 1883, reached the column of smoke from Krakatoa. **Later the haze only dropped slightly, then remained at about the same height, and then dropped considerably from November to December**.

Longer series of individual observers, such as Rollo Russell's in England, O. Jesse's in Berlin and Meldrum's on Mauritius, i.e. in very remote places, also lead to results very similar to the above general averages from all observations. **The haze would have dropped by 15,000 m between August 1883 and February 1884**.

Direct cite from English translation of Pernter (1889, Meteorologische Zeitschrift: pages 456 and 457)
(word count is 115 words for 4 sentences at top-of-page, and 119 words for 2 paras below the Table.)

→ steep Krakatau aerosol descent (32km → 24km 1[st] weeks)
very similar to that observed after Hunga
(consistent with water vapour cooling forced descent)

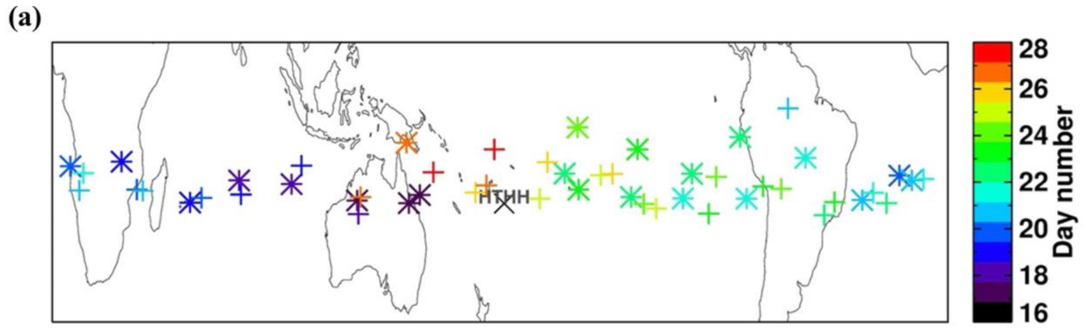

Taha et al. (2022, GRL)

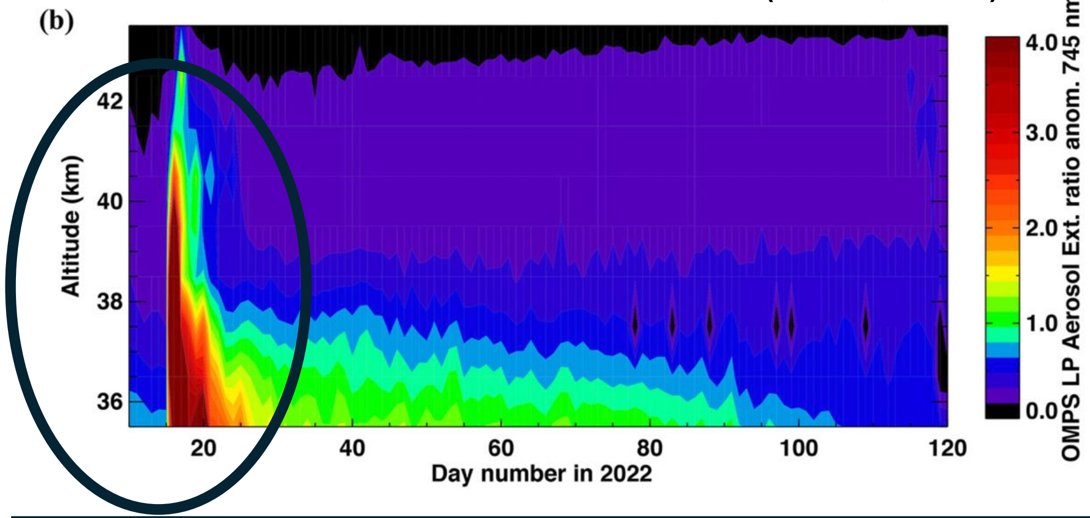

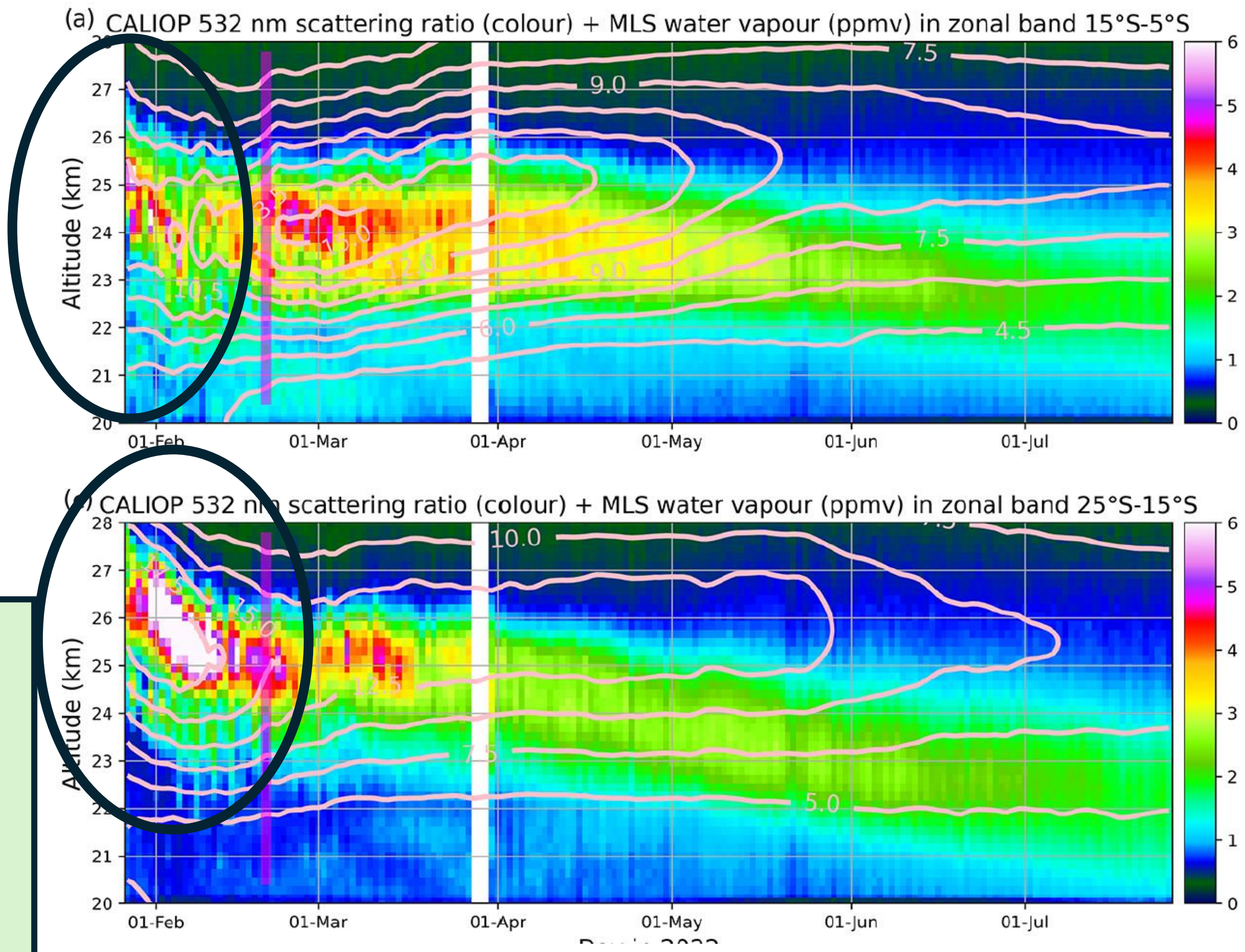

Legras et al. (2022, GRL, Figure 3)

Summary re: Hunga and Krakatau

→ Krakatau thought to have also emitted a very large co-emission of H2O to stratosphere → ~500Tg (offset part of surface cooling ~40Tg of SO_2 ?)

→ H_2O injection into stratosphere from Krakatau via pyroclastic flow entering the ocean (different to Hunga's shallow underwater setting)

→ Initial descent of Krakatau aerosol from purple twilight consistent with strong water vapour cooling